COMPOSITE PLATES AND THEIR LAY-UP SOLUTIONS LEADING TO HIGH BUCKLING AND POST-BUCKLING RESISTANCE

Sergey Selyugin

AIRBUS Operations GmbH, Kreetslag 10, 21129 Hamburg, Germany

e-mail: sergey.selyugin@airbus.com

Abstract

At the beginning of the present paper, the post-buckled composite plates are examined. The plates have a symmetric lay-up. The layer orientation angles vary in a point-wise way or in a plate-wise way. The von Karman theory describes a plate behavior. For a plate stiffness maximization problem the first-order optimality conditions are derived. In the conditions, the essential roles play the mid-plane principal strains and the principal curvatures. The optimality conditions may lead to a co-axiality of some structural tensors. Analytical examples illustrate the solutions of such types. Further, several numerical examples are presented. In the examples, the plates are loaded by shear and have the high buckling-resisting ability also. A significant conclusion of the paper is that in the properly designed lay-up the outermost layers and the innermost layers play different roles. The former ones withstand mainly buckling, and the latter ones withstand mainly post-buckling. The innermost layers have the orientation angle rather close to 0°. The weight reduction opportunities are demonstrated.

Keywords: composite plates; post-buckling; lay-up.

1. INTRODUCTION

Post-buckling of thin composite plates attracts the attention of numerous researchers, working in various modern application areas. Among these applications are the aerospace, the automotive, the marine, and the civil ones. According to design practice in composite structures, the account of the load-carrying capability “above buckling” gives an opportunity of extra weight saving, as compared to existing traditional design.

Composite plates are part of the considerable number of structures in the above applications. The loading applied to the plates is a combination of compression and shear. The compression dominates for the structures similar to the upper panels of an airplane wing structure. As the examples of known structures designed for pure shear, one may indicate airplane wing ribs and spars. In some cases, the shear-loaded plates should withstand the same level of shear loading applied in the direct and opposite loading direction. Such cases are inherent in the aerospace structures like the ribs and the spars of the vertical tail plane, the fuselage skin panels, etc. As a rule, the shear-loaded plates have the so-called angle-ply symmetric lay-up. For example, buckling is not allowed in airplane structures in the case of loading up to the so-called limit loads (LL) and may be allowed for the loading level between the limit loads and the so-called ultimate loads (UL). The latter loads are 1.5 times higher than the limit loads.

When optimizing the composite plate, an engineer, in fact, does his best to save the structural weight, the material cost, and the production time. Due to that, the optimization problems for the composite plates attract the considerable attention at the design phase. The lay-up optimization problem is one of them requiring a solution at the beginning of the design process.

Since the last decade of the previous century, numerous papers dealt with the lay-up optimization of composite plates. The non-exhaustive list [1]-[22] contains the important publications devoted to the post-buckling analysis and optimization. In the list, there are also several latest papers. The foundations of the post-buckling theory are described in [23]. Other interesting publications may be found in the references of the above-indicated papers.

All published papers in the area are devoted to numerical optimization studies. In the majority of available textbooks, no bending-twisting coupling and no shear-extension coupling are considered (see, e.g., [24]). The couplings are mainly taken into account in journal papers. Various optimization criteria are used, in particular: end-shortening, maximal compression strain, maximal deflection, estimated stiffness, etc.

Among papers considering a description of the post-buckling stiffness, the paper [6] should be indicated. In the paper, the compressed post-buckled orthotropic laminated plates are considered. The plate behavior is described by two equations: the von Karman equation, and the strain compatibility equation. The equations are the ones for the deflections and for the Airy stress function. The solutions of the equations are determined numerically. For the numerical process, the deflections are described by a sum of several trigonometric terms. The latter terms satisfy the boundary conditions. The estimated value of the post-buckling stiffness in each direction is equal to the derivative of the corresponding load with respect to the compression strain. The maximization of the initial post-buckling stiffness is based on the estimation and is performed numerically.

"Quick answer" approximations are the result of the closed-form post-buckling solutions. As references, the papers [3], [11], [12] may be indicated. In the papers, the shear-loaded structures are considered.

The numerical perturbation approach to post-buckling analysis should be mentioned as rather popular. For references one may refer to [3], [8], and [15].

Several papers are devoted to approximate solutions. The ones devoted to the finite strip approach [9] may be indicated in this regard.

Several papers, in particular, [1] and [10], describe software projects. The projects deal with post-buckling analysis and optimization of aerospace structures.

The dissertation [19] considers, in particular, aspects of plate post-buckling. The plates under discussion are made of the specially orthotropic balanced material, with a) maximum (compression) strain as the failure criterion, b) blending constraints (not more than four neighboring plies of the same angle), c) discrete set of ply angles. It is noticed, that failure-optimized and buckling-optimized lay-ups may be considerably different in some cases of loading. The wing-box optimization is also considered.

The paper [20] minimizes the post-buckling dynamic response and maximizes the buckling load, using a special convolution function for two criteria. Numerical examples are considered. In general, the particular objectives conflict with each other necessitating a multi-objective formulation. The latter formulation includes the post-buckling energy and the critical buckling load.

The paper [21] considers a discrete version of the firefly algorithm (DFA). The algorithm is adapted to lay-up optimization of post-buckled composite structures.

In [22], the authors present a novel method of design optimization. The method is a gradient-based one and is intended for optimization of post-buckling performance. The considered structures are made of composite material. The post-buckling analysis of the structures is based on Koiter's asymptotic method. The corresponding design sensitivities of the Koiter's factors are derived, for further usage in the gradient-based optimization. Subsequently, new design optimization formulations are presented; they are based on the sensitivities. The proposed optimization formulations are intended for optimization of post-buckling stability. In conclusion, the square plate and the curved panel illustrate the concept.

A considerable number of works is devoted to the VAT composites. The studies were initiated in the last decade of the previous century in Virginia Tech, Delft University, Bristol University, and other locations. For references, one may use the most recent papers like [16-

18]. In such papers, the advantages of VAT composites for post-buckling load-carrying capacity are explored numerically and compared to the so-called “quasi-isotropic” or “straight fiber” solutions. As a rule, the ply orientation angles to be considered are linear functions of a coordinate.

In [16], the balanced VAT laminates are numerically studied, using the Tsai-Wu failure criterion and controlling end-shortening and maximal deflection.

In [17], the difference of the post-buckling behavior in case of positive and negative shear loading of VAT plates is demonstrated and discussed.

The today’s opinion of the composite optimization community based on numerical and approximate studies is: the surface plies dominate the buckling events whilst the inner plies dominate the postbuckling (see [30]).

Potentially, having more degrees of freedom, the VAT solutions are more promising, as compared to the conventional “straight fiber” solutions. On the other hand, the drawback of the VAT approach is that there is no known theoretical basis for verifying, validating, and explaining the solutions obtained.

In available publications, no influence of flexural and plane anisotropy on optimal lay-up in post-buckling is considered theoretically. The numerical experience till now covers a considerable number of various examples and requires creating a generalized understanding.

The present paper deals with the composite plates loaded with shear. The plates are assumed to have no rotational edge stiffness.

There are two main targets of the paper. The first one is theoretical; the task is to reveal the regularities of the optimal lay-ups both of “variable ply orientation angle” and of “straight fiber” composite plates in post-buckling. The second target is to explore the “straight fiber” post-buckling solutions numerically. In our opinion, the potential of the “straight fiber” lay-up design is not exhausted. Moreover, the latter lay-ups are much cheaper in production, as compared to the VAT ones.

The present paper deals with the plates of symmetric lay-up. The optimality conditions to be derived are necessary for obtaining an understanding of the specifics, inherent in numerical solutions. The conditions are derived for a simplified optimization formulation only, with the objective function being the structural potential energy. After that, numerical examples of composite plates are presented using the “best lay-up choice” criterion of maximal compression strain. The used simplifications in a problem formulation allow reaching our goals easier. In our opinion, the maximal deflection may indicate the possible closeness of failure and may estimate the level of contour forces. Due to that, it is useful to watch the maximal deflections during numerical optimization.

Some theoretical and numerical results of the paper are of an academic nature; their objective is to obtain a better understanding of the “best lay-up” structure.

The organization of the present paper is as follows.

Section 1 contains an introduction and a short literature review.

Section 2 deals with the theoretical consideration of composite plate post-buckling in the case of single loading. The first order necessary optimality conditions for the structural stiffness maximization problem are derived, analyzed and discussed.

Section 3 presents various numerical examples for the “straight fiber” plates and discuss the corresponding results. The purpose of the Section is to identify the trends inherent in the composite plates in post-buckling.

Section 4 contains a discussion of the whole paper content.

Section 5 presents the conclusions of the paper.

2. THEORETICAL CONSIDERATION

2.1 ENERGY FORMULATION

The theoretical consideration deals with post-buckled thin, flat composite plate. The Classical Laminated Plate Theory (CLPT) [26] describes the behavior of the plate, using the Kirchhoff assumptions. The plate is of symmetric lay-up and contains $2N$ tape layers (for simplicity, the laminates with the odd number of layers are outside the discussion; the generalization to the case is straightforward). The boundary condition types are simple support or clamped. As known from practice, the simple support conditions model properly the single-row riveting; the double-row riveting is well-modeled by the clamping conditions. The contour of the plate is a piece-wise smooth one. The Green strain tensor contains both linear and nonlinear terms (w.r.t. deflections). The plate coordinate system is (x, y); the loads are the plane loads.

The kinematic variational principle (the structural potential energy stationary principle), together with the strain compatibility condition, describe the plate post-buckling behavior (see [24], and [25] Section 8).

The variational principle for the composite plates under the above assumptions is formulated in the following way. The quantities (u, v, w) are the corresponding plate displacements in the Cartesian coordinates (x, y, z), respectively; w is the out-of-plane deflection. The corresponding components of the Green strain tensor in the plate mid-plane, with an account of nonlinear terms, are:

$$e_{xx0} = \frac{\partial u}{\partial x} + \frac{1}{2}\left(\frac{\partial w}{\partial x}\right)^2 \; ; \; e_{yy0} = \frac{\partial v}{\partial y} + \frac{1}{2}\left(\frac{\partial w}{\partial y}\right)^2 \; ; \; e_{xy0} = \frac{1}{2}\left(\frac{\partial u}{\partial y} + \frac{\partial v}{\partial x} + \frac{\partial w}{\partial x}\frac{\partial w}{\partial y}\right) \tag{1}$$

The components of the tensor of the mid-plane curvatures:

$$k_x = -\frac{\partial^2 w}{\partial x^2} \; ; \; k_y = -\frac{\partial^2 w}{\partial y^2} \; ; \; k_{xy} = -\frac{\partial^2 w}{\partial x \partial y} \tag{2}$$

The quantities in (1), (2) create the following vectors (below we follow the engineering approach of [26]):

$$\overline{\varepsilon^0}^T = \left(e_{xx0}, e_{yy0}, 2e_{xy0}\right) \; ; \; \overline{k}^T = \left(k_x, k_y, 2k_{xy}\right) \tag{3}$$

where the superscript T means a transposition.

In the case of large rotations and moderate deflections (see [25], Section 8) the strain potential energy is:

$$\Pi = \int dS \left(\frac{1}{2} \overline{\varepsilon^0}^T A \overline{\varepsilon^0} + \frac{1}{2} \overline{k}^T D \overline{k} \right) \tag{4}$$

where A and D are the (3*3) matrices describing 2D-mid-plane behavior and bending of the plate [26], the vectors $\overline{\varepsilon^0}, \overline{k}$ are determined in (3). The integration in (4) is performed over the plate mid-plane surface.

The structural potential energy is:

$$U = \int dS \left(\frac{1}{2} \overline{\varepsilon^0}^T A \overline{\varepsilon^0} + \frac{1}{2} \overline{k}^T D \overline{k} \right) - W \tag{5}$$

where W is the potential of external "dead" forces depending on the forces, on the displacements at the loaded part of the external boundary, on the external pressure (if any), and on the corresponding deflections within the plate. The kinematic variational principle states that in equilibrium the structure satisfies

$$\delta U = \delta \Pi - \delta W = 0 \tag{6}$$

for all kinematically admissible displacements (u, v, w).

The principle (6) leads to the equilibrium equation for the deflections w and for the stress flows N_x, N_y, N_{xy} within the plate (see [25] for the usual sign convention). The plate deflections and the mid-plane strains must also satisfy the compatibility equation:

$$\frac{\partial^2 e_{xx0}}{\partial y^2} + \frac{\partial^2 e_{yy0}}{\partial x^2} - 2\frac{\partial^2 e_{xy0}}{\partial x \partial y} = \left(\frac{\partial^2 w}{\partial x \partial y} \right)^2 - \frac{\partial^2 w}{\partial x^2} \frac{\partial^2 w}{\partial y^2} \tag{7}$$

2.2 POINT-WISE OPTIMALITY CONDITIONS

Fig. 1 shows the orthotropic lamina (see [26], Section 2.6). The stress tensor components within the lamina in the coordinates (*x, y*) are:

$$\begin{pmatrix} \sigma_x \\ \sigma_y \\ \tau_{xy} \end{pmatrix} = \begin{bmatrix} \overline{Q}_{11} & \overline{Q}_{12} & \overline{Q}_{16} \\ \overline{Q}_{12} & \overline{Q}_{22} & \overline{Q}_{26} \\ \overline{Q}_{16} & \overline{Q}_{26} & \overline{Q}_{66} \end{bmatrix} \begin{pmatrix} \varepsilon_x \\ \varepsilon_y \\ 2\varepsilon_{xy} \end{pmatrix} \tag{8}$$

where $\overline{Q}$ is the lamina stiffness matrix, and $\varepsilon_x, \varepsilon_y, \varepsilon_{xy}$ are the lamina infinitesimal strain tensor components.

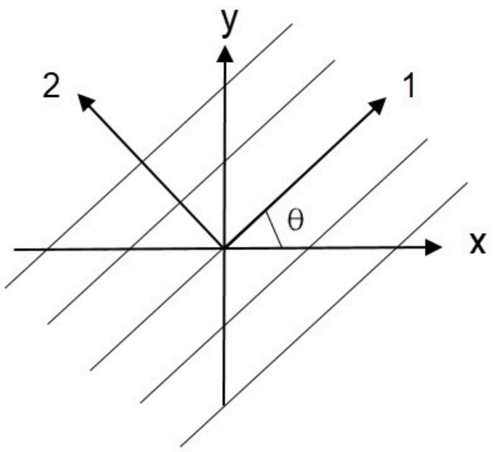

Fig. 1. Orthotropic lamina with material orientation (1, 2).

The components of the lamina stiffness matrix are (see [26], Section 2.6):

$$
\begin{aligned}
\overline{Q}_{11} &= U_1 + U_2 \cos 2\theta + U_3 \cos 4\theta \\
\overline{Q}_{12} &= U_4 - U_3 \cos 4\theta \\
\overline{Q}_{22} &= U_1 - U_2 \cos 2\theta + U_3 \cos 4\theta \\
\overline{Q}_{16} &= \frac{1}{2} U_2 \sin 2\theta + U_3 \sin 4\theta \\
\overline{Q}_{26} &= \frac{1}{2} U_2 \sin 2\theta - U_3 \sin 4\theta \\
\overline{Q}_{66} &= \frac{1}{2} (U_1 - U_4) - U_3 \cos 4\theta
\end{aligned}
\tag{9}
$$

where U_1, U_2, U_3, U_4 are the elastic constants of the orthotropic layer following from the formulae:

$$
\begin{aligned}
U_1 &= \frac{1}{8}\left(3Q_{11} + 3Q_{22} + 2Q_{12} + 4Q_{66}\right) \\
U_2 &= \frac{1}{2}\left(Q_{11} - Q_{22}\right) \\
U_3 &= \frac{1}{8}\left(Q_{11} + Q_{22} - 2Q_{12} - 4Q_{66}\right) \\
U_4 &= \frac{1}{8}\left(Q_{11} + Q_{22} + 6Q_{12} - 4Q_{66}\right)
\end{aligned}
\tag{10}
$$

and

$$
\begin{aligned}
Q_{11} &= \frac{E_1}{1 - \nu_{12}\nu_{21}} \\
Q_{12} &= \frac{\nu_{12} E_2}{1 - \nu_{12}\nu_{21}} \\
Q_{22} &= \frac{E_2}{1 - \nu_{12}\nu_{21}} \\
Q_{66} &= G_{12}
\end{aligned}
\tag{11}
$$

where $E_1, E_2, G_{12}, \nu_{12}, \nu_{21}$, respectively, are two elastic moduli for directions 1 and 2, the shear modulus, and two Poisson ratios.

According to (9), the derivatives of the lamina stiffness matrix $\overline{Q}_{ij}$ w.r.t. the orientation angle Θ are:

$$\frac{d\overline{Q}_{11}}{d\theta} = -2U_2 \sin 2\theta - 4U_3 \sin 4\theta = -4\overline{Q}_{16}$$
$$\frac{d\overline{Q}_{22}}{d\theta} = 2U_2 \sin 2\theta - 4U_3 \sin 4\theta = 4\overline{Q}_{26} \tag{12}$$
$$\frac{d\overline{Q}_{12}}{d\theta} = 4U_3 \sin 4\theta = 2(\overline{Q}_{16} - \overline{Q}_{26})$$

Determination of A_{ij} and D_{ij} via the lamina parameters is performed according to the general formulas [26], *ij=11, 12, 22, 16, 26, 66*:

$$A_{ij} = \sum_{k=1}^{N} \left(\overline{Q}_{ij}\right)_k \left(z_k - z_{k-1}\right) \tag{13}$$

$$D_{ij} = \frac{1}{3}\sum_{k=1}^{N} \left(\overline{Q}_{ij}\right)_k \left(z_k^3 - z_{k-1}^3\right) \tag{14}$$

where z_k, z_{k-1} are the top and the bottom *z*-coordinates of the layer (*z*=0 corresponds to the mid-plane).

The derivatives of the stiffness matrices *A, D* w.r.t. lamina angles θ_k are, *ij=11, 12, 22; k=1,...,N*:

$$\frac{dA_{ij}}{d\theta_k} = (z_k - z_{k-1})\frac{d\left(\overline{Q}_{ij}\right)_k}{d\theta_k}$$
$$\frac{dD_{ij}}{d\theta_k} = \frac{1}{3}(z_k^3 - z_{k-1}^3)\frac{d\left(\overline{Q}_{ij}\right)_k}{d\theta_k} \tag{15}$$

where θ_k is the layer orientation angle.

Below we consider the structural potential energy *U* from (5) as a measure of the structural stiffness. The goal of lay-up optimization is to maximize the post-buckling stiffness value, varying the ply orientation angles point-wise or plate-wise.

In this sub-Section, we consider the point-wise case and assume, that the lamina orientation angles θ_k are smooth functions of the mid-plane location (*x, y*).

Following the usual variational procedure and taking into account the variational principle (6), we obtain the first order necessary optimality conditions in the case of point-wise variations of the layer orientation angles. The maximization of the structural stiffness means that the first variation of U with respect to the orientation angles is equal to zero.

$$\delta U = \delta U\Big|_{\substack{A-non-\text{var}\,ied \\ D-non-\text{var}\,ied}} + \delta U\Big|_{(u,v,w)-non-\text{var}\,ied} = 0 \qquad (16)$$

The first item in (16) is equal to zero due to (6). Hence, from the second item we obtain a relation for the orientation angle of k-th layer at a current point:

$$\frac{dU}{d\theta_k} = \left.\frac{\partial \Pi}{\partial \theta_k}\right|_{u,v,w=const} = 0\,, \;\; k=1,\ldots,N \qquad (17)$$

Further, we calculate the first items in (4), (17) (the items correspond to the mid-plane 2D-strains), in the axes of the principal 2D mid-plane strains $\varepsilon_1, \varepsilon_2$ (the whole tensor is determined in (1)), where $\varepsilon_1 \geq \varepsilon_2$. The second items in (4), (17) (the items correspond to the plate bending and twisting), we calculate in the axes of the principal plate curvatures k_1, k_2, where $k_1 \geq k_2$. Making necessary transformations in (17) and remembering that the absolute value of the Jacobian of a transition from the principal mid-plane strain coordinates to the principal curvature coordinates is equal to 1.0 (the transition is a simple rotation), we obtain:

$$\frac{1}{2}\left\{(\varepsilon_1, \varepsilon_2)\begin{bmatrix} \dfrac{dA_{11}^{pr.str.}}{d\theta_k} & \dfrac{dA_{12}^{pr.str.}}{d\theta_k} \\ \dfrac{dA_{12}^{pr.str.}}{d\theta_k} & \dfrac{dA_{22}^{pr.str.}}{d\theta_k} \end{bmatrix}\begin{pmatrix}\varepsilon_1 \\ \varepsilon_2\end{pmatrix}\right\} + \frac{1}{2}\left\{(k_1, k_2)\begin{bmatrix} \dfrac{dD_{11}^{pr.cur.}}{d\theta_k} & \dfrac{dD_{12}^{pr.cur.}}{d\theta_k} \\ \dfrac{dD_{12}^{pr.cur.}}{d\theta_k} & \dfrac{dD_{22}^{pr.cur.}}{d\theta_k} \end{bmatrix}\begin{pmatrix}k_1 \\ k_2\end{pmatrix}\right\} = 0 \qquad (18)$$

where *pr.str.*, *pr.cur.* correspond to the principal mid-plane strain axes and to the principal curvature axes.

Analyzing (18), we consider at the beginning the first item there.

Substituting in (18) the relations (12)-(15), we obtain for every k-th layer, k=1,…,N:

$$\left\{\begin{array}{l} \varepsilon_1^2\left[-2U_2\sin 2(\theta_k-\varphi) - 4U_3\sin 4(\theta_k-\varphi)\right] + \\ + \varepsilon_2^2\left[2U_2\sin 2(\theta_k-\varphi) - 4U_3\sin 4(\theta_k-\varphi)\right] + 2\varepsilon_1\varepsilon_2 4U_3\sin 4(\theta_k-\varphi) \end{array}\right\}\frac{1}{2}\left(z_k - z_{k-1}\right) \qquad (19)$$

where φ is the angle between the global x axis and the ε_1 axis.

Analogously the second item gives for every k-th layer, k=1,…,N:

$$\left.\begin{cases} k_1^2\left[-2U_2\sin 2(\theta_i-\psi)-4U_3\sin 4(\theta_i-\psi)\right]+ \\ +k_2^2\left[2U_2\sin 2(\theta_i-\psi)-4U_3\sin 4(\theta_i-\psi)\right]+2k_1k_2 4U_3\sin 4(\theta_i-\psi) \end{cases}\right\}\frac{1}{6}\left(z_k^3-z_{k-1}^3\right) \tag{20}$$

where ψ is the angle between the global x axis and the k_1 axis.

The sum of (19) and (20), equated to zero, is the first order necessary optimality condition at every layer, k=1,...,N

$$\begin{aligned} &\left.\begin{cases} \varepsilon_1^2\left[-2U_2\sin 2(\theta_k-\varphi)-4U_3\sin 4(\theta_k-\varphi)\right]+ \\ +\varepsilon_2^2\left[2U_2\sin 2(\theta_k-\varphi)-4U_3\sin 4(\theta_k-\varphi)\right]+2\varepsilon_1\varepsilon_2 4U_3\sin 4(\theta_k-\varphi) \end{cases}\right\}\frac{1}{2}\left(z_k-z_{k-1}\right)+ \\ &+\left.\begin{cases} k_1^2\left[-2U_2\sin 2(\theta_i-\psi)-4U_3\sin 4(\theta_i-\psi)\right]+ \\ +k_2^2\left[2U_2\sin 2(\theta_i-\psi)-4U_3\sin 4(\theta_i-\psi)\right]+2k_1k_2 4U_3\sin 4(\theta_i-\psi) \end{cases}\right\}\frac{1}{6}\left(z_k^3-z_{k-1}^3\right)=0 \end{aligned} \tag{21}$$

As we see, the conditions for every layer are highly nonlinear ones. Transforming (21), we obtain:

$$\begin{aligned} &2\sin 2(\theta_k-\varphi)\left.\begin{cases} \varepsilon_1^2\left[-U_2-4U_3\cos 2(\theta_k-\varphi)\right]+ \\ +\varepsilon_2^2\left[U_2-4U_3\cos 2(\theta_k-\varphi)\right]+8\varepsilon_1\varepsilon_2 U_3\cos 2(\theta_k-\varphi) \end{cases}\right\}\frac{1}{2}\left(z_k-z_{k-1}\right)+ \\ &+2\sin 2(\theta_k-\psi)\left.\begin{cases} k_1^2\left[-U_2-4U_3\cos 2(\theta_k-\psi)\right]+ \\ +k_2^2\left[U_2-4U_3\cos 2(\theta_k-\psi)\right]+8k_1k_2U_3\cos 2(\theta_k-\psi) \end{cases}\right\}\frac{1}{6}\left(z_k^3-z_{k-1}^3\right)=0 \end{aligned} \tag{22}$$

and finally, dividing by $-\left(z_k-z_{k-1}\right)4U_3$:

$$\begin{aligned} &\sin 2(\theta_k-\varphi)\left[\frac{U_2}{4U_3}\left(\varepsilon_1^2-\varepsilon_2^2\right)+\left(\varepsilon_1-\varepsilon_2\right)^2\cos 2(\theta_k-\varphi)\right]+ \\ &+\sin 2(\theta_k-\psi)\left[\frac{U_2}{4U_3}\left(k_1^2-k_2^2\right)+\left(k_1-k_2\right)^2\cos 2(\theta_k-\psi)\right]\frac{1}{3}\left(z_k^2+z_kz_{k-1}+z_{k-1}^2\right)=0 \end{aligned} \tag{23}$$

As we see, the explicit dependence on the layer z location comes through the last multiplier of the second item. The dependence on material comes through the parameter $\frac{U_2}{4U_3}$. It is interesting to note that all multipliers of the trigonometric functions are non-negative.

Analyzing (23), one may say also that the innermost layers and the outermost layers play different roles there. In particular, it follows from the first item in (23) that the innermost layers are mostly sensitive to the principal 2D-strains and their principal directions. As to the outermost layers, they are mostly sensitive (due to z^2 multiplier of the second item) to the principal plate curvatures and their principal directions.

If we make a sum of (22) for all k and keep in mind (12)-(17), we obtain the following united condition

$$\left[A_{16}^{pr.str.}\varepsilon_1^2 - A_{26}^{pr.str.}\varepsilon_2^2 - \left(A_{16}^{pr.str.} - A_{26}^{pr.str.}\right)\varepsilon_1\varepsilon_2\right] + \left[D_{16}^{pr.cur.}k_1^2 - D_{26}^{pr.cur.}k_2^2 - \left(D_{16}^{pr.cur.} - D_{26}^{pr.cur.}\right)k_1k_2\right] = 0 \tag{24}$$

or, after using the definitions of the stiffness matrices A and D, the relation with the clear physical meaning

$$N_{xy}^{pr.str.}(\varepsilon_1 - \varepsilon_2) + M_{xy}^{pr.cur.}(k_1 - k_2) = 0 \tag{25}$$

The relation (25) is a linear combination of the optimality conditions (22) or (23) and, hence, also it is the optimality condition uniting the ones for every layer. The first item in (25), if considered separately as equal to zero, means that the nonlinear mid-plane strain tensor is co-axial with the stress flow tensor (or, for $\varepsilon_1 \neq \varepsilon_2$, the shear flow in the principal strain axes is equal to zero). The second item in (25), if considered separately as equal to zero, means that the tensor of the curvatures is co-axial with the moment tensor (or, for $k_1 \neq k_2$, the twisting moment in the principal curvature axes is equal to zero).

It should be noted that the result, in the case of an orthotropic plate with a point-wise orthotropic orientation, follows from (25) with the number of layers N=1.

2.3 PLATE-WISE OPTIMALITY CONDITIONS

In the case of the plate-wise variation of the layer fiber angles, the first order necessary optimality conditions for every layer are different from (23). The conditions in the case mean that the integral of (22) or (23) over the plate is equal to zero.

A generalization of (25) for the case is

$$\int_S dxdy\left[N_{xy}^{pr.str.}(\varepsilon_1-\varepsilon_2)+M_{xy}^{pr.cur.}(k_1-k_2)\right]=0 \tag{26}$$

where S is the plate mid-plane surface.

A generalization of (23) to the plate-wise case is written as follows:

$$\int_S dxdy\left[\begin{array}{l}\sin 2(\theta_k-\varphi)\left[\dfrac{U_2}{4U_3}\left(\varepsilon_1^2-\varepsilon_2^2\right)+\left(\varepsilon_1-\varepsilon_2\right)^2\cos 2(\theta_k-\varphi)\right]+\\ +\sin 2(\theta_k-\psi)\left[\dfrac{U_2}{4U_3}\left(k_1^2-k_2^2\right)+\left(k_1-k_2\right)^2\cos 2(\theta_k-\psi)\right]\dfrac{1}{3}\left(z_k^2+z_kz_{k-1}+z_{k-1}^2\right)\end{array}\right]=0 \tag{27}$$

Analysis of the optimality conditions (obtained in the sub-Section) leads to the following conclusions. The first conclusion corresponds to the case of loads slightly higher than the buckling level. In the case, the second item (related to the curvatures) of the optimality conditions plays the key role. The reason is that the order of magnitude of the first (2D-strain) item in (25), (26) is the same as the order of magnitude of the product of the second (bending-twisting) item and the quantity $\bar{w}^2/t^2$. In the latter ratio the quantities $t,\bar{w}$ are the plate thickness and the maximal deflection, with the following inequality being valid $\bar{w}^2/t^2 \ll 1$. The second conclusion corresponds to the case of the loads considerably higher than the buckling level. In the case, we may propose the following conjecture: the role of the first item (related to the 2D-strains) of the optimality conditions becomes comparable to the role of the second item.

In particular, the so-called diagonal tension behavior [24] of the shear loaded post-buckled structure, in our opinion, is, a confirmation of the conjecture (to some extent).

It follows from the above-obtained optimality conditions that the key drivers of the lay-up optimality for the innermost plies are the mid-plane strains, and the key drivers for the outermost plies are the mid-surface curvatures.

It is interesting to mention that (see [29]) the lay-up of the maximal upper estimate of the first buckling value corresponds to the second item in (23)-(27). In the case of pre-buckling, the lay-up solution with maximal stiffness value corresponds to the first item in (23)-(27).

Concluding this Section, we note that optimality conditions of other types are not under discussion here. The conditions are beyond the scope of the present paper.

3. NUMERICAL EXAMPLES

3.1 PRELIMINARY CONSIDERATION

In the present paper, we use the FE method (with isoparametric quadrilateral rectangular four-node elements) for both buckling and post-buckling analysis. The buckling problem is solved, basing on a Lanczos method. The nonlinear solution steps (above buckling) consist of gradual load increments, iterations with convergence tests for acceptable equilibrium error, and stiffness matrix updates. The iterative process is based on the quasi-Newton's method and on the line search. The stiffness matrix updates are performed occasionally to improve the computational efficiency and may be overridden at the user's discretion.

Rectangular composite plates are considered (see Fig. 2). Fig. 2 shows the positive shear loading direction. The letters C and E indicate the lower corner points. The origin of the x-y coordinate system is located at the point C. We use the simple support boundary conditions (as the most conservative ones) in numerical examples everywhere below. It means that the contour out-of-plane displacements are not allowed.

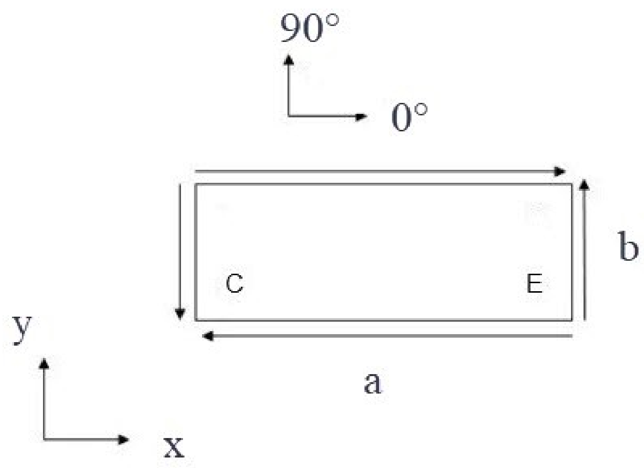

Fig. 2. Rectangular plate.

Fig. 3 illustrates the boundary support conditions used in the FEM analysis of buckling and post-buckling. We identified during below numerical studies that the support reactions at the corner points C and E are negligible.

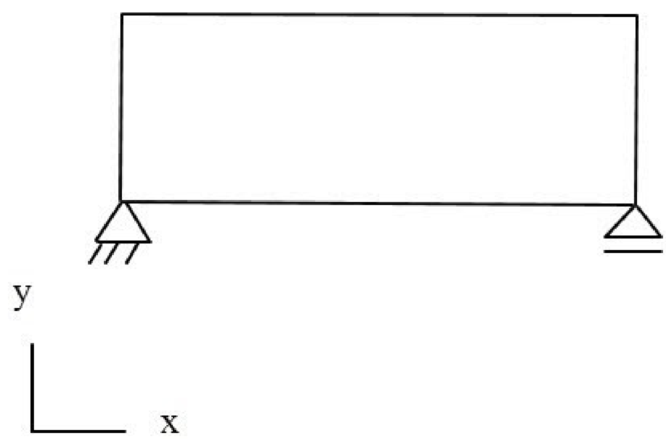

Fig. 3. Boundary support conditions.

The initial imperfection of the post-buckling analysis is equal to 1.E-05 times the transverse displacement of the first buckling mode. The similar approach was successfully used in [18]. In other papers like [17], the multiplier was 1% of the plate thickness. In the present paper, we perform a direct spot-check of the influence of maximal initial imperfection on results obtained. No influence on post-buckling analysis results exists in the case of a switch from 1.E-05 to 1.E-03 factors. Nevertheless, we use the value 1.E-05 everywhere below.

In post-buckling, it is assumed that there is no switch between buckling modes. It is also supposed that the post-buckling is developed to a moderate extent. The latter assumption is necessary for the von Karman moderate deflection approach to be valid.

At the bottom of sub-Section 3.3, we consider a possibility to use the so-called "straight line" boundary conditions. The conditions are modeled by bars, contouring the composite plate of 2 mm thickness. It is identified that the reinforcement increases the buckling level. As to the post-buckling behavior, the influence of the innermost layers to the plate behavior exists in the case.

After some trials, we chose the level of loading above buckling for every configuration of the paper basing on the necessity of having maximal compression strain level not higher than 5000 micro strains (see [18]). The criterion is of frequent use in aerospace applications [18]. It is clear that the criterion is only an approximation of the real failure conditions. Such conditions must also include consideration of the junctions between the plate and the edge member. If the maximal post-buckling plate deflection value becomes lower (for the obtained solutions) compared to the maximal deflection of the known solutions, then the fact may implicitly require a decrease of edge junction forces. In the present paper, we watch the deflections from this viewpoint and demonstrate the decrease of the maximal plate deflection in the solutions obtained, as compared to the angle-ply or the "equal buckling" [29] solutions.

Direct search of the best lay-up solutions consists of calculating the structural behavior at the nodes of the 1° grid of ply orientation angles.

Talking about the below-presented examples, we should say that the loading intensity (and the value of the so-called post-buckling ratio) correspond to an acceptable buckling and post-buckling behavior. Saying "acceptable behavior" we mean that the maximal compression strain value in post-buckling is not higher than 5000 micro strains.

3.2 NUMERICAL APPROACH USED FOR BUCKLING AND POST-BUCKLING ANALYSIS

First, we present some comparative study to verify our approach.

The paper [27] is devoted to the post-buckling analysis of composite plates under shear conditions. One of the examples of the paper is a boron-epoxy plate of the dimensions 0.25*0.25 m and symmetric angle-ply lay-up [45°, 135°]s. The plate is of 2.5 mm thickness, it is loaded by a positive shear loading, and has the simple support boundary conditions. The ply characteristics are: E_{11}=206.9 GPa, E_{22}=20.7 GPa, the Poisson ratio ν_{12}=0.3, the shear modulus G_{12}=5.2 GPa. The applied shear loading is 40000 N/m. In [27], the results are presented in non-dimensional forms, using the non-dimensional load factor $q = \frac{N_{xy} b^2}{E_{22} h^3}$ (where N_{xy} is the applied shear flow and b is the plate width 0.25 m) and the non-dimensional deflection normalized to the plate thickness h.

Convergence studies performed in the present work for eigenvalue analysis of the above-described boron-epoxy plate gives the eigenvalue of 2.553 in the case of the mesh 40x40 and of 2.549 in the case of the mesh 80x80. Hence, the mesh 40x40 is good enough for the determination of the eigenvalue as 2.55 (from the aerospace structural engineer point of view).

Comparison with results of [27] for the post-buckling analysis shows the high quality of the approach used in the present paper, see Fig 4. In Fig. 4 the shear flow is normalized to 2.55*40000 N/m.

The buckling level for the example in [27] equals 2.65 (for obtaining the total load the value should be multiplied to 40000 N/m). According to the present FEM approach, the buckling level is 4% lower.

Comparison of results obtained according to the present approach for two mesh densities (40*40 and 80*80) shows the same level of 8.3 mm for maximum deflection (at the plate center) in the case of loading 1.75*2.55*40000 N/m = 178500 N/m.

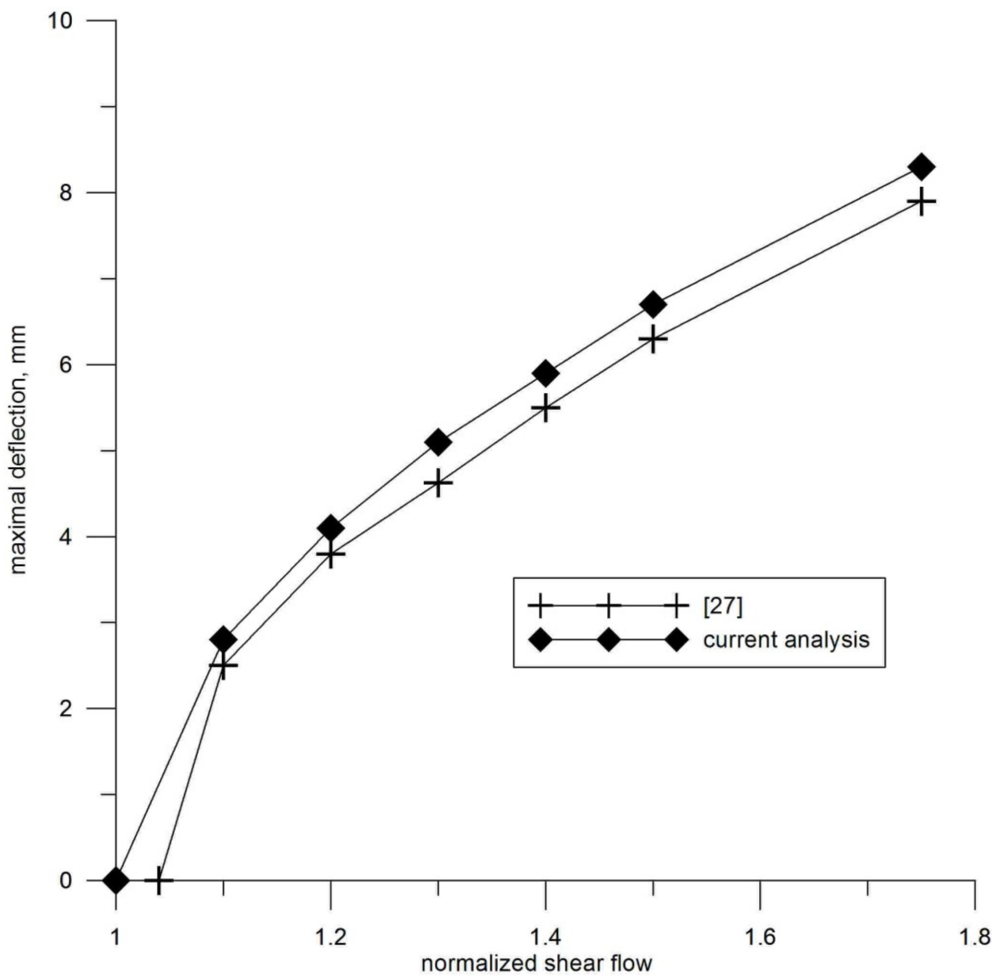

Fig. 4. Maximal deflection at the plate center, comparison with [27].

Fig. 4 demonstrates that the central deflections in our analysis are higher to some extent, as compared to ones of [27]. In our opinion, this fact is a consequence of the lower precision in [27], where 25 terms of some expansion presenting the solution were used. Due to that, the plate in [27] is “stiffer” than the plate in our analysis.

The consideration verifies our approach.

Further, we consider rectangular composite plates with the aspect ratio *a/b*=2., 3., and 5. The thickness values are equal to 2 mm and 3 mm. The width of the plate *b* everywhere in the paper is equal to 0.2 m (200 mm).

The plates are made of the tape material T300/5208 with the thickness 0.000125 m (0.125 mm) and the properties shown in Table 1. In our FEM approach to the buckling and the post-buckling analysis, the cell size is 5*5 mm. The cell dimensions follow from the solution precision analysis conducted for various cell dimensions.

Manufacturer	**Fiber**	**Matrix**	**Form**
Hexcel	T300 Carbon	5208 Epoxy	UD
E11, GPa	**E22**, GPa	**G12**, GPa	**ν12**
181	10.3	7.17	0.28

Table 1. T300/5208 Carbon/Epoxy Unidirectional Prepreg

3.3 LONG PLATE UNDER SHEAR LOADING IN SINGLE LOADING DIRECTION

We consider a long rectangular composite plate with the aspect ratio *a/b*=5 and the thickness value 2 mm.

The symmetric plate-wise lay-up variants discussed in the sub-Section contain 16 layers. The plate load is the shear flow 50000 N/m (called hereinafter the scale level), multiplied by some factor.

According to the paper [28], the best orientation against buckling for a long plate under the positive-directed shear loading is 120° for all layers (of course, the result is of an academic nature). The buckling eigenvalue in the case of *a/b*=5 equals 2.83. Below in the sub-Section, we perform a comparison of the lay-up configurations, considering the plate loaded in the positive direction only up to the level of the so-called post-buckling ratio (PBR) equal to 1.2. This means, that the total shear flow is equal to 169800 N/m = 1.2*2.83*50000 N/m. The choice of PBR value 1.2 follows from the necessity to stay within the region of moderate deflections (the assumption, together with the large rotations, is a basis of the von Karman plate theory). Further, we analyze the structural behavior of the above plate for a variety of the lay-up solutions.

The following example basing on the $[[120°]_8]_S$ plate is considered: two close-to-mid-plane layers change their orientation angles together (in fact, there are four such layers due to lay-up symmetry). The angle variation creates a plate with orientations $[[120°]_6,[\theta]_2]_S$, where the angle θ should be determined numerically from a direct minimization (approximately) of the maximal 2-D compression strain and, if possible, of the maximal deflection also. The number of two of the varied innermost layers is chosen deliberately, hoping that the change of these layer orientation angles may influence the buckling eigenvalue to a small extent.

Fig. 5 demonstrates the post-buckled shape of the plate $[[120°]_8]_S$. We obtain the values of 12.2 mm maximal deflection and of 7.0E-03 maximal compression 2-D strain.

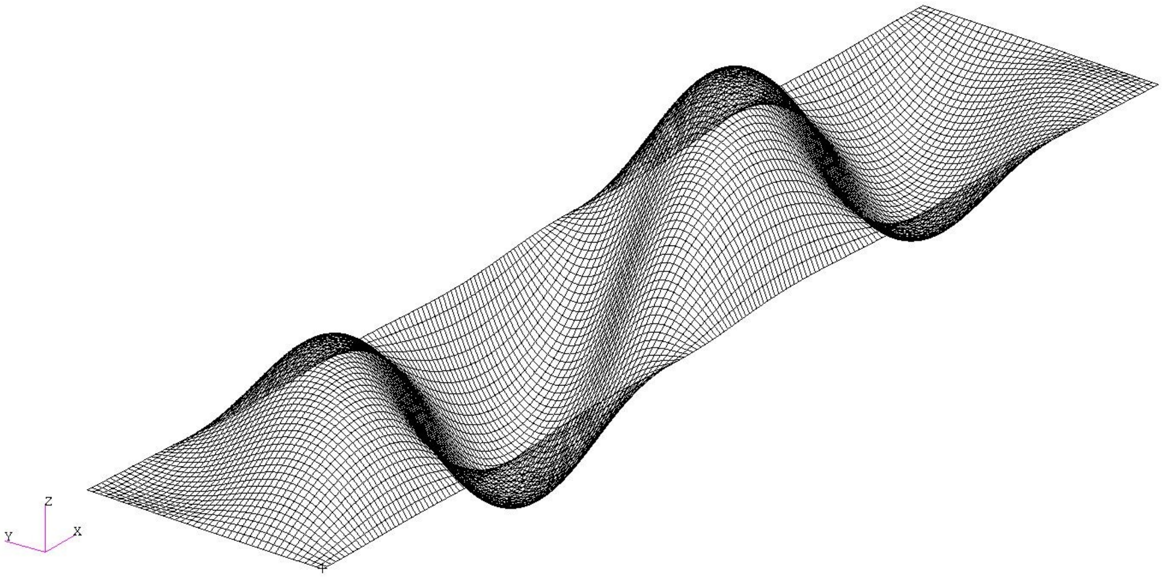

Fig. 5. Post-buckled shape, *a/b*=5, lay-up $[[120°]_8]_S$

The plate $[[120°]_6,[-4°]_2]_S$ is the result of the numerical search. The result corresponds to the lay-up leading to a minimum of the maximal compression strain value. The latter plate has the maximal compression strain of 4.9E-03 (70% of the strain for the pure $[[120°]_8]_S$ plate), the maximal deflection of 6.9 mm (57% of the deflection for the pure $[[120°]_8]_S$ plate), and the eigenvalue of 2.80. As we see, the eigenvalue goes slightly down about 1%, as expected. It is also interesting, that the angle between the X axis and the maximal mid-plane principal strain direction (tension) is distributed within the plate in the narrow range between 60° and 52°, being concentrated closer to 52°.

The lay-up of the plate $[[120°]_6,[4°]_2]_S$ follows from the numerical search, leading to a minimum of the maximal deflection. The plate has the maximal deflection of 6.6 mm (54% of the deflection for the pure $[[120°]_8]_S$ plate), the maximal compression strain of 5.2E-03 (74% of the strain for the pure $[[120°]_8]_S$ plate), and the lowest buckling eigenvalue of 2.80.

It is clear that the difference in the above two lay-up results and their characteristics is rather small. The obtained results mean, that in practical design one may use $[[120°]_6,[0°]_2]_S$

solution, giving the nearly lowest deflection of 6.7 mm and maximal compression strain of 5.0E-03 values.

Fig. 6 presents the deflected surface of the $[[120°]_6,[-4°]_2]_S$ plate. Observation of Figs. 5, 6 leads to a conclusion that the deflected surface is similar to the case of $[[120°]_8]_S$.

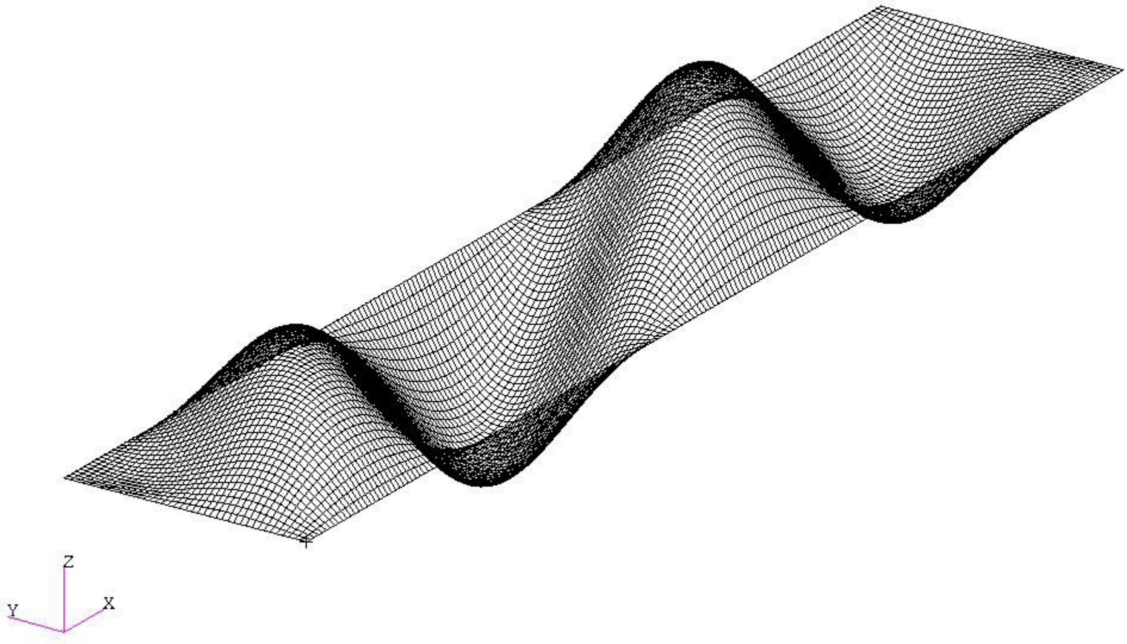

Fig. 6. Post-buckled shape, *a/b*=5, lay-up $[[120°]_6,[-4°]_2]_S$.

Table 2 presents the results for the plates $[[120°]_8]_S$ and $[[120°]_6,[0°]_2]_S$. the Table demonstrate the locations of the maximal deflection points, the locations of the maximal compression strains, and the directions of the principal strains. As we see, the changes in the locations are small, but the values come down considerably. It is also visible from the Table that there is some location symmetry.

Lay-up	Maximal deflection, mm	Maximal compression strain	Coordinates (x, y), mm	Minor principal strain direction, angle with X in °	Lower (L) or upper (U) plate surface
$[[120°]_8]_S$	12.2		(625., 100.)		
$[[120°]_8]_S$	-12.2		(375., 100.)		
$[[120°]_8]_S$		7.0E-03	(487.5, 32.5)	-47.7	U
$[[120°]_8]_S$		7.0E-03	(512.5, 167.5)	-47.7	L
$[[120°]_6,[0°]_2]_S$	6,7		(630., 100.)		
$[[120°]_6,[0°]_2]_S$	-6,7		(370., 100.)		
$[[120°]_6,[0°]_2]_S$		5.0E-03	(517.5, 172.5)	-40.4	U
$[[120°]_6,[0°]_2]_S$		5.0E-03	(482.5, 27.5)	-40.4	L

Table 2. Detailed results, positive loading, $a/b = 5$, $t = 2$ mm

Analyzing the results of Table 2, we see that both the maximal deflection and the maximal compression strain value come down considerably (55% and 71% of the corresponding values of the solution $[[120°]_8]_S$), with the orientation angle value being higher than in the case of $[[120°]_8]_S$. The locations of peak values at the Table have very small changes. The orientation angle of maximal compression strain changes to some extent.

Summarizing the above results, one may say that the innermost layer orientations influence the post-buckling behavior considerably, with the buckling eigenvalue being changed to a small extent.

Some consideration should be made to a possibility to use the so-called straight-edge condition. If we consider the plate $[[120°]_6,[0°]_2]_S$ as contoured by aluminum bars with 5 mm

* 5 mm cross-section, then the shear buckling eigenvalue in the case is equal to 3.03 and the eigenmode is similar to one of the non-contoured case of Fig. 5. The bars have the non-zero axial stiffness and in-plane bending stiffness values. Simple support conditions are still used for the plate. For the plate of $[[120°]]_{8S}$ lay-up with the same bar contouring and boundary conditions the eigenvalue is equal to 3.06 (8% difference with the original value of 2.83 for the lay-up $[[120°]]_{8S}$ without the contouring). Applying the shear load higher than buckling load, namely, up to the level of 1.2*3.06*50000 N/m = 183600 N/m, we reach the following post-buckling parameters:

- the lay-up $[[120°]_6,[0°]_2]_S$: the maximal compression strain of 5.4E-03 and the maximal deflection of 7.4 mm;
- the lay-up $[[120°]]_{8S}$: the maximal compression strain of 7.7E-03 and the maximal deflection of 13.6 mm.

Note that with the rise of the bar cross-section up to 10 mm*10 mm the eigenvalues (for the plate lay-ups $[[120°]]_{8S}$ and $[[120°]_6,[0°]_2]_S$) increase considerably and become 4.15 and 4.11, respectively. The edges of the contour in post-buckling with the shear loading of 1.1*4.11*50000 N/m are not straight yet (the value of loading is chosen to lead to the maximal compression strains not much higher than 5.E-03). For the plate lay-up $[[120°]]_{8S}$ the maximal deflection and the maximal compression strain values are of 8.7 mm and of 6.3E-03, respectively. For the plate lay-up $[[120°]_6,[0°]_2]_S$, the maximal deflection and the maximal compression strain values are of 5.0 mm and of 5.4E-03, respectively. The conclusion following from the analysis of the contour-reinforced plates (modeling a possibility to use the straight-edge conditions) is 1) the conditions lead to a very high buckling eigenvalue, and 2) in post-buckling above the value the influence of the innermost layer orientations on improving the post-buckling behavior still exists.

In our opinion, the simple support boundary conditions (used in the numerical examples of the present paper) allow us to explore the pure plate structural work and to identify the specific features of the plate behavior.

Elastic restraint of edges against rotation over them and its influence on post-buckling behavior should be explored from the above standpoint in further papers.

3.4 PLATES UNDER SHEAR LOADING IN TWO OPPOSITE LOADING DIRECTIONS

In the sub-Section, we study numerically the plates with various aspect ratio and thickness values (with 1° direct optimization search accuracy, as before). The plate loads are the shear loads applied in two opposite loading directions. For the so-called "equal buckling level" solution we use the results taken from [29]. In the analysis of the sub-Section, the buckling resistance (lowest buckling eigenvalue level) is also taken into account. Namely, the search of the best orientation angles for the innermost layers is performed starting from the "equal buckling" solution. In the further description, we talk about the solution with high resistance to both buckling and post-buckling. This means that in the search the maximal post-buckling compression strain value reaches its lowest value. The value of the maximal deflection is also watched.

3.4.1 Plate a/b=5, thickness 2mm

We consider three variants of the plate with the post-buckling behavior. The variants are: the angle-ply one $[[45°,135°]_4]_S$ (the eigenvalues of 1.29 and of -1.66), the variant $[[74°,134°]_4]_S$ with approximately equal buckling resistance in both loading directions (the eigenvalues of 1.69 and of -1.70), the variant having ply orientations of the second variant with the orientations of the two innermost layers being chosen to maximize the post-buckling performance. It is assumed that in the third case the buckling eigenvalues will not be changed considerably.

The loading is made with PBR=1.5 applied to the level of buckling equal to 1.29; this means that the shear flow value (maximal) is equal to 1.5*1.29*50000 N/m = 1.935*50000 N/m=96750 N/m.

The third variant leads to the solution $[[74°,134°]_3,[9°]_2]_S$, with the eigenvalues being equal to 1.69 and -1.69. Table 3 gives an overview of the results obtained. We see that the bottom line of the Table presents a solution of a high quality, from both maximal strain level and maximal deflection value standpoint.

	Positive loading 1.935=1.5*1.29			Negative loading 1.935		
Laminate	max deflec-tion, mm	max compres-sion strain	min eigen-value	max deflec-tion, mm	max compres-sion strain	min eigen-value
$[[45°,135°]_4]_S$	14.8	9.2E-03	1.29	8.4	4.5E-03	-1.66
$[[74°,134°]_4]_S$, "equal buckling" lay-up	5.3	3.8E-03	1.69	4.0	4.2E-03	-1.70
$[[74°,134°]_3,[9°]_2]_S$	3.2	2.4E-03	1.69	2.6	2.4E-03	-1.69

Table 3. Results for the plate with thickness 2 mm and *a/b*=5.

The corresponding post-buckling shapes for the positive loading are shown in Figs. 7-9.

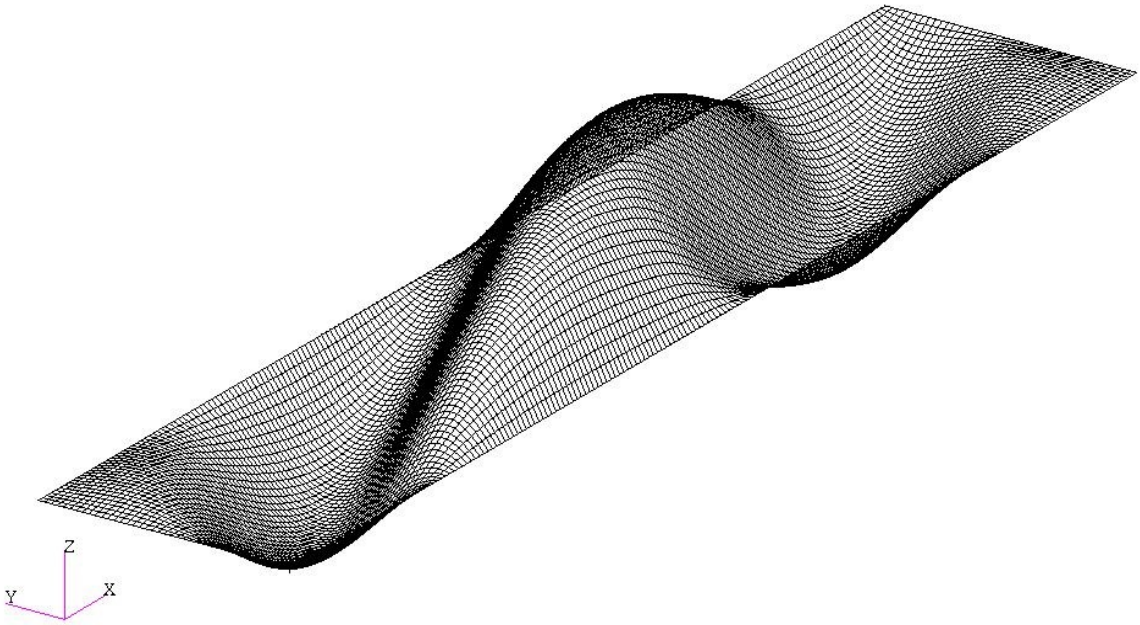

Fig. 7. Post-buckled shape, angle-ply lay-up, *a/b*=5, positive loading.

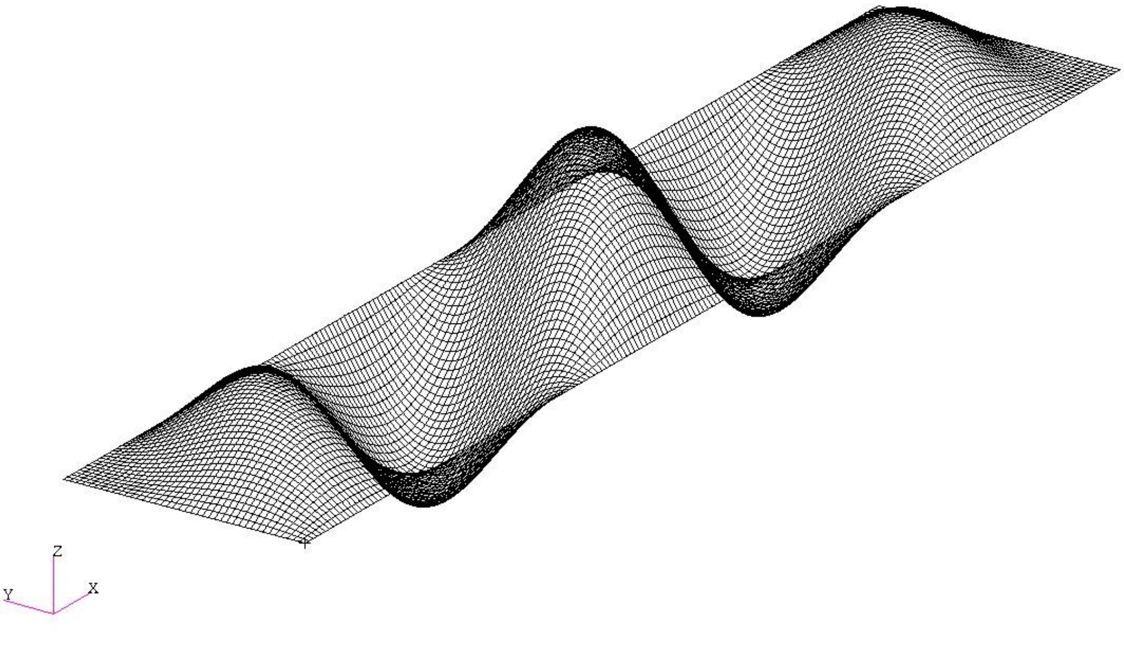

Fig. 8. Post-buckled shape, $[[74°,134°]_4]_S$, *a/b*=5, positive loading.

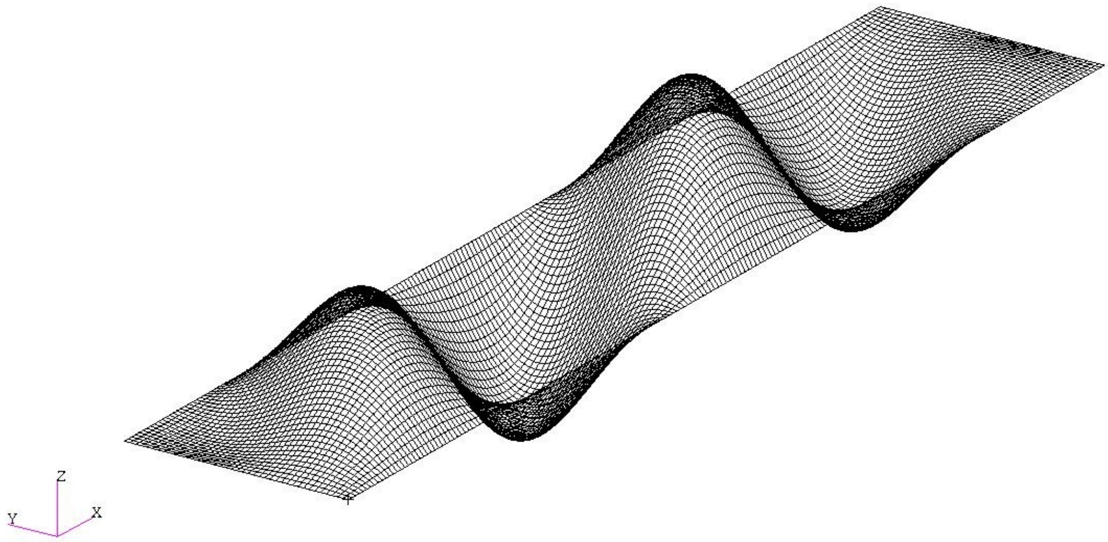

Fig. 9. Post-buckled shape, $[[74°,134°]_3,[9°]_2]_S$, a/b=5, positive loading.

More detailed information on the results for the above plates is given in Table 4. The results corresponding to the negative loading are specially marked by the words "negative loading".

Lay-up	Maximal deflection, mm	Maximal compression strain	Coordinates (x, y), mm	Minor principal strain direction, angle with X in °	Lower (L) or upper (U) plate surface
$[[45°,135°]_4]_S$	14.8		(500., 100.)		
$[[45°,135°]_4]_S$		9.2E-03	(627.5, 142.4)	-75.5	L
$[[74°,134°]_4]_S$	5.3		(500., 100.)		
$[[74°,134°]_4]_S$ negative loading		4.2E-03	(402.5, 172.5)	37.6	U
$[[74°,134°]_3,[9°]_2]_S$	3.2		(600., 100.)		
$[[74°,134°]_3,[9°]_2]_S$		2.4E-03	(492.5, 42.5)	-55.5	L

Table 4. Detailed results for the plate with thickness 2 mm and a/b=5.

It follows from above three Figs. that the post-buckled shape of all three variants is different from each other.

Analysis of Tables 3, 4 and Figs. 7-9 leads to the conclusions that for the variant $[[74°,134°]_3,[9°]_2]_S$ the maximal deflection (regardless of the loading direction) is about 22% of the deflection for the variant $[[45°,135°]_4]_S$. The maximal compression strain of the variant $[[74°,134°]_3,[9°]_2]_S$ is about 26% of the strain for the angle-ply lay-up. Hence, the variant $[[74°,134°]_3,[9°]_2]_S$ has a considerably better post-buckling performance with nearly the same level of buckling, as compared to the "equal buckling level" variant $[[74°,134°]_4]_S$.

For the variant $[[74°, 134°]_3, [9°]_2]_S$, an analysis of the influence of the initial perturbation shape on the post-buckling performance is performed. The first, the second, and the third buckling eigenmodes for both loading directions are used. Moreover, the first and the second modes (for both loading directions) correspond to a doubled eigenvalue (both 1.69 and -1.69). As to the third modes, they are isolated from the corresponding first and second ones. Analysis of the post-buckling behavior leads to slightly lower (within 5%) maximal compression strain values and maximal deflections, as compared to the case of using the first buckling mode. Nevertheless, the post-buckled shapes are different from each other. The author intends to publish a more detailed analysis and an explanation of the interesting effect in a separate paper.

3.4.2 Plate a/b=3, thickness 2 mm

In the sub-Section, we consider three variants of the plate with the post-buckling behavior. The variants are: the angle-ply one $[[45°,135°]_4]_S$ (the eigenvalues of 1.39 and of -1.79), the variant $[[74°,136°]_4]_S$ with approximately equal buckling resistance in both loading directions (the eigenvalues of 1.75 and of -1.74), the variant having ply orientations of the above second variant for all plies except the orientations of the two innermost layers. The latter orientations are chosen to maximize the post-buckling performance (assuming that the buckling eigenvalues will not be changed considerably). The words "to maximize the post-buckling performance" mean to reach the lowest levels of the maximal compression strain (and the maximal deflection, if possible).

The loading is made using PBR=1.5 applied to the level of buckling equal to 1.39; this means that the shear flow value equals 1.5*1.39*50000 N/m = 2.085*50000 N/m = 104250 N/m.

The third variant leads to the solution $[[74°, 136°]_3,[9°]_2]_S$ with the buckling eigenvalues equal to 1.74 and -1.73. Table 5 gives an overview of the results obtained.

	Positive loading 2.085 (=1.5*1.39)			Negative loading 2.085		
Laminate	max deflection, mm	max compres-sion strain	min eigen-value	max deflection, mm	max compres-sion strain	min eigen-value
$[[45°,135°]_4]_S$	9.9	7.8e-03	1.39	6.6	3.4E-03	-1.79
$[[74°,136°]_4]_S$, "equal buckling" lay-up	6.2	4.5E-03	1.75	5.0	5.2E-03	-1.74
$[[74°,136°]_3,[9°]_2]_S$	3.6	2.8E-03	1.74	3.1	2.8E-03	-1.73

Table 5. Results for the plate with thickness 2 mm and *a/b*=3.

It follows from the Table that the trend in Table 5 is the same as in Table 3. Namely, there is a decrease of the maximal compression strain and the maximal deflection values from top to bottom. Hence, the variant $[[74°,136°]_3,[9°]_2]_S$ has a considerably better post-buckling performance with nearly the same level of buckling as compared to the "equal buckling level" variant $[[74°,136°]_4]_S$. Note that the obtained values at the bottom line of Table 3 are slightly higher than the corresponding ones of Table 3.

The plots of the post-buckling shape and the locations of maximal deflections and compression strain values are similar to the plots and results of the previous sub-Section. Due to that, they are not presented here.

Analysis of Table 5 leads to the conclusions that: 1) the maximal compression strain for the variant $[[74°,136°]_3,[9°]_2]_S$ (regardless of the loading direction) is about 36% of the strain for the angle-ply lay-up, 2) the maximal deflection for the variant $[[74°,136°]_3,[9°]_2]_S$ is about 36% of the deflection for the variant $[[45°,135°]_4]_S$. Hence, the variant $[[74°,136°]_3,[9°]_2]_S$ has a considerably better post-buckling performance with nearly the same level of buckling, as compared to the "equal buckling level" variant $[[74°,136°]_4]_S$.

3.4.3 Plate a/b=3, thickness 3 mm

We consider here three variants of the plate with the post-buckling behavior. The variants are: the angle-ply $[[45°,135°]_6]_S$ one (the eigenvalues of 4.92 and of -5.84), the variant $[[70°,130°]_6]_S$ with nearly equal buckling resistance in both loading directions (the eigenvalues of 6.08 and of -6.06), the variant differing from the second one due to the orientations of three innermost layers. The latter orientations are chosen to maximize the post-buckling performance (assuming that the buckling eigenvalues will not be changed considerably) from the point of view of making the lowest level of the maximal compression strain.

Note that for the plates with considerable thickness the post-buckling ratio used should be taken lower than 1.5, for decreasing the maximal compression strain level up to a more acceptable level.

The examples of such analysis of the considered plate with PBR=1.3 and the loads equal to 1.3*4.92*50000 N/m = 6.396*50000 N/m = 319800 N/m are given in Table 6 below.

	Positive loading 6.396 (=1.3*4.92)			Negative loading 6.396		
Laminate	max deflec-tion, mm	max compres-sion strain	min eigen-value	max deflec-tion, mm	max compres-sion strain	min eigen-value
$[[45°,135°]_6]_S$	10.9	1.2E-02	4.9	6.1	6.2E-03	-5.8
$[[70°,130°]_6]_S$, "equal buckling" lay-up	4.6	5.1e-03	6.1	4.2	8.1E-03	-6.1
$[[70°,130°]_4,70°,[9°]_3]_S$	3.0	4.1E-03	6.0	2.5	3.8E-03	-6.1

Table 6. Results for the plate with thickness 3 mm and *a/b*=3.

The Table shows that the first and the second lines are not acceptable due to high compression strains, but the bottom line looks acceptable. Comparing the bottom line with the angle-ply solution in the case of positive loading, the maximal compression strain level becomes 34% of the one for the angle-ply solution and the maximal deflection becomes about 28% of the one for the angle-ply solution. In the case of negative loading, the corresponding values are 61% and 41%, respectively.

The plots of the post-buckled shapes, the location of the maximal deflections, and the location of the maximal compression strain are similar to the ones of the sub-Section 3.4.1 and are not presented here.

Observing the results of sub-Sections 3.4.1-3.4.3, one may say that the plates with *a/b* higher than (or equal to) 3 may be considered as the long plates. Obviously, the conclusion is valid within the scope of the present paper.

3.4.4 Plate a/b=2, thickness 2 mm

The plate discussed now is a short one. We consider three variants of the plate with the post-buckling behavior. The variants are: the angle-ply one $[[45°,135°]_4]_S$ (the eigenvalues of

1.56 and of -2.00), the variant $[[74°,140°]_4]_s$ with nearly equal buckling resistance in both loading directions (the eigenvalues of 1.84 and of -1.82), the variant having the orientations of the plies like in the above second variant except the orientations of the two innermost layers. The latter orientations are chosen to maximize the post-buckling performance from the point of view of making the lowest level of the maximal compression strain.

The loading is made with PBR=1.5 applied to the level of buckling equal to 1.56; this means that the shear flow value is equal to 1.5*1.56*50000 N/m = 2.34*50000 N/m = 117000 N/m.

The third variant leads to the solution $[[74°, 140°]_3,[18°]_2]_s$ with the buckling eigenvalues equal to 1.83 and -1.82. Table 7 gives an overview of the results obtained.

	Positive loading 2.34 (=1.5*1.56)			Negative loading 2.34		
Laminate	max deflection, mm	max compres-sion strain	min eigen-value	max deflection, mm	max compres-sion strain	min eigen-value
$[[45°,135°]_4]_s$	9.6	6.2E-03	1.56	5.6	3.0E-03	-2.00
$[[74°,140°]_4]_s$, "equal buckling" lay-up	5.6	5.4E-03	1.84	5.0	6.5E-03	-1.82
$[[74°,140°]_3,[18°]_2]_s$	3.4	3.4E-03	1.83	3.3	3.2E-03	-1.82

Table 7. Results for the plate with thickness 2 mm and *a/b*=2.

The corresponding post-buckling shapes for the positive loading are shown in Figs. 10-12.

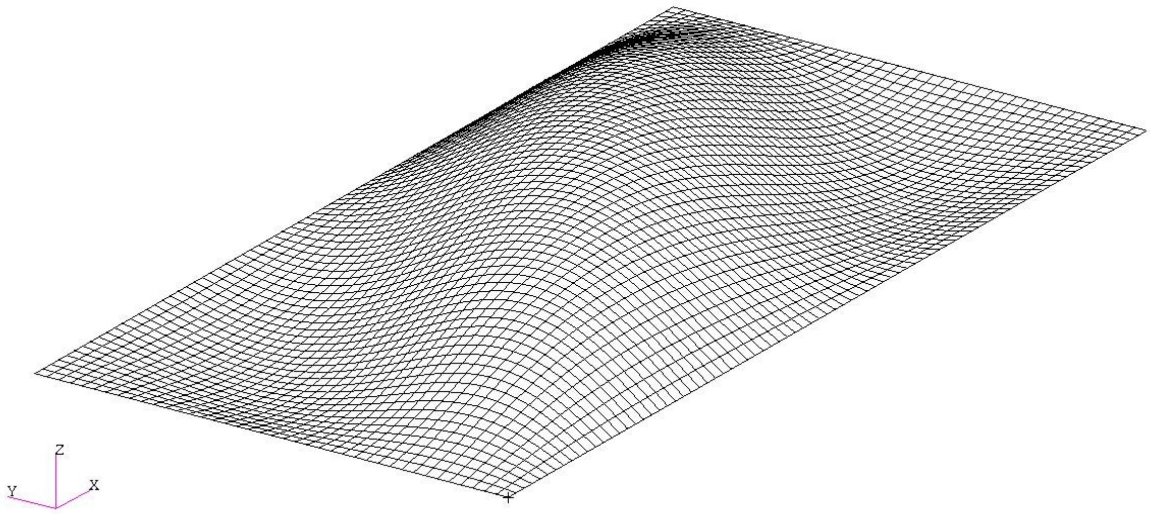

Fig. 10. Angle-ply lay-up $[[45°,135°]_4]_S$, positive loading, a/b=2.

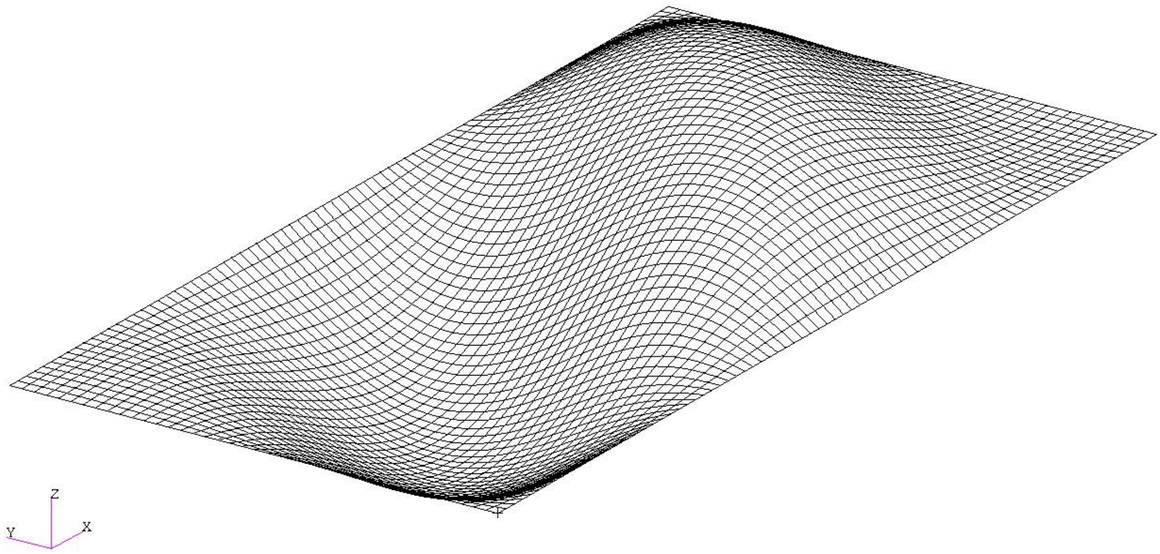

Fig. 11. “Equal-buckling” lay-up $[[74°,140°]_4]_S$, positive loading, a/b=2.

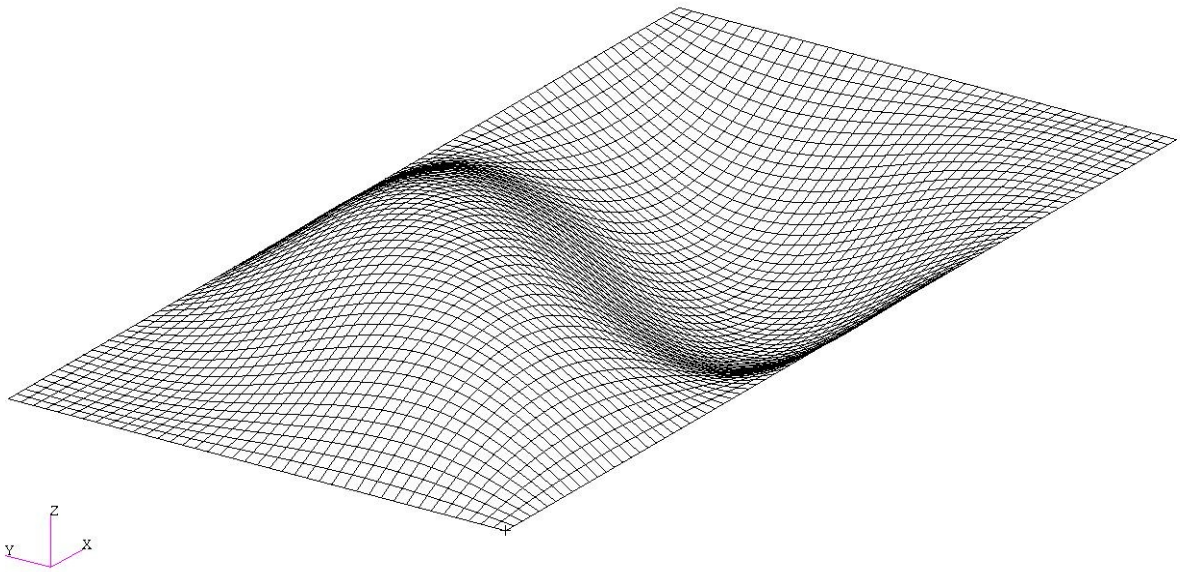

Fig. 12. Lay-up $[[74°,140°]_3,[18°]_2]_S$, positive loading, a/b=2.

It follows from Figs. 10-12 that the post-buckled shapes for the variants are considerably different from each other.

Table 8 shows the locations of maximal deflection and maximal compression strain for the lay-up variants (with both positive and negative shear loading). In the Table, we specially mark the lines corresponding to the negative loading.

Lay-up	Maximal deflection, mm	Maximal compres-sion strain	Coordinates (x, y), mm	Minor princi-pal strain di-rection, angle with X in °	Lower (L) or upper (U) plate surface
$[[45°,135°]_4]_S$	9.6		(200., 100.)		
$[[45°,135°]_4]_S$		6.2E-03	(67.5, 37.5)	-65.7	L
$[[74°,140°]_4]_S$	5.6		(285., 105.)		
	-5.6		(115., 95.)		
$[[74°,140°]_4]_S$ negative loading		6.5E-03	(222.5, 22.5)	36.1	L
$[[74°,140°]_4]_S$ negative loading		6.5E-03	(177.5, 177.5)	36.1	U
$[[74°,140°]_3,[18°]_2]_S$	3.4		(115., 105.)		
$[[74°,140°]_3,[18°]_2]_S$	-3.4		(285., 95.)		
$[[74°,140°]_3,[18°]_2]_S$		3.4E-03	(212.5, 162.5)	-56.1	L
$[[74°,140°]_3,[18°]_2]_S$		3.4E-03	(187.5, 37.5)	-56.1	U

Table 8. Detailed results, a/b=2, t=2 mm

Analysis of Tables 7, 8 and Figs. 10-12 leads to a conclusion that the variant $[[74°,140°]_3,[18°]_2]_S$ has the maximal compression strain value (regardless of the loading direction) even higher than the value for the negative loading and the angle-ply solution, but nevertheless lower than the limit of 5.E-03. We see also that the strain distribution is considerably different from one of the angle-ply solution (the orientations of the maximal compression strains are considerably different).

The maximal deflection in the variant $[[74°,140°]_3,[18°]_2]_S$ is about 61% of the deflection in the variant $[[45°,135°]_4]_S$.

As a resumè, we may say that the variant $[[74°,140°]_3,[18°]_2]_S$ has a considerably better post-buckling performance with nearly the same level of buckling, as compared to the "equal buckling level" variant $[[74°,140°]_4]_S$.

Basing on the angle-ply plate solution, the results of below Table 9 demonstrate the weight reduction opportunities following from the better post-buckling performance of the obtained lay-ups (*a/b*=2, thickness 2 mm). The level of loading is equal to 1.4*1.56*50000 N/m = 2.184*50000 N/m (it is lower than the above-used level to make the angle-ply design nearly acceptable). One 18° ply is removed from the center of the plate stacking. As a result of that, we have the 6.25% weight reduction (the total number of plies is changed from 16 to 15).

	Positive loading 2.184 (=1.4*1.56)			Negative loading 2.184		
Laminate	max deflec-tion, mm	max compres-sion strain	min eigen-value	max deflection, mm	max compres-sion strain	min eigen-value
$[[45°,135°]_4]_S$, t=2mm	8.3	5.1E-03	1.56	3.9	2.1E-03	-2.00
$[[74°,140°]_3,[18°]_3, [140°,74°]_3]$, t=1.875mm	4.5	4.2E-03	1.50	4.2	4.6E-03	-1.51

Table 9. Weight reduction opportunity demonstration; plate with *a/b*=2.

4. DISCUSSION

The lay-up choice criterion of the present paper is the minimum of the maximal compression strain. The criterion of the minimum of the maximal deflection may be applied in the post-buckling regime to see whether or not the failure has been initiated. The latter criterion was used in the literature for several decades. The maximal deflection criterion is also useful for decreasing the averaged level of contour forces at the plate attachments. The strain criterion is important for indication of the potential failure location.

The switch between buckling modes may considerably influence the post-buckling behavior. On the other hand, it is known that in practice the post-buckling ratio is not so high.

For example, in the aerospace applications, the ratio should not be higher than 1.5. Moreover, the structural test practice in the applications demonstrates that such switches are rather rare and their account is not so significant. In our opinion, the approach of the present paper ("no switches") is acceptable.

It is obtained from the theoretical analysis that for the solutions with the highest post-buckling stiffness the orientation angles of the innermost layers are determined mainly by the 2D-plane principal strain values and their directions. The orientation angles of the outermost layers in the case are mainly determined by the plate principal curvature values and their directions.

In our opinion, the results of the sub-Section 3.3 give a significant image describing the nearly optimal lay-up of the long plate loaded by single loading. The plate has a high resistance to buckling and post-buckling. The lay-up contains a few innermost layers of about 0° and other layers with 120° orientation angles.

Some recommendations follow from the numerical analysis of the shear-loaded post-buckled composite plates. The plates have various opposite loadings, various thickness values, and various aspect ratio values. The recommendations are: the presence of some innermost layers with moderate (up to, say, 20°) orientation angles improves the plate post-buckling load-carrying capacity, as compared to the plates designed for resisting buckling only. It means that there are three important directions of the ply orientations. In our opinion, the result may be described by the superposition of two following lay-up solutions.

The first one corresponds to the positive shear loading and has a few 0° innermost layers plus other layers with the orientations 120°. The second solution is the mirrored first one (relatively to the 90° line). The superposed solution is rotated to some extent due to bending-twisting and shear-extension coupling. The following schematic of the lay-up creation (Fig. 13) within the scope of the present paper may be proposed (the innermost layers are shown by the dashed lines):

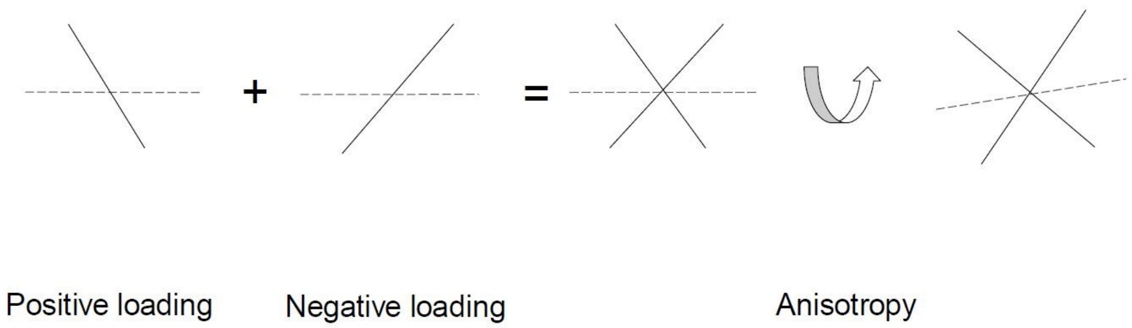

Fig. 13. The schematic of the optimized lay-up creation.

The final step of the schematic shows that the lay-ups of all examples of sub-Section 3.4 are slightly rotated in the counter-clockwise direction.

There is no practical lay-up difference for the plates with the aspect ratio values of 3 and 5. Therefore, a plate with a/b=3 may be considered as a long plate.

A considerable advantage of the obtained solutions over the classical angle-ply lay-up is identified. The result may be beneficial for the lay-up design of composite plates and panels.

It is identified that with the decrease of the plate aspect ratio there is an increase of the innermost layer orientation angles.

5. CONCLUSIONS

The conclusions follow from the performed lay-up study:

- The first order necessary optimality conditions for the post-buckling stiffness maximization problem are highly nonlinear ones;
- The optimality conditions contain two terms. One of them corresponds to the plate bending-twisting, and another one corresponds to the mid-plane nonlinear strains;

- The principal mid-plane strain lines and the principal curvature lines play an important role in the conditions;
- The united point-wise optimality condition contains two terms. The first term corresponds to the bending-twisting and equals zero when the tensor of curvatures is co-axial with the moment tensor. The second term corresponds to the mid-plane strains and equals zero when the mid-plane strain tensor is co-axial with the mid-plane stress flow tensor;
- The presented numerical examples clarify specific features of the optimized lay-up solutions. The solutions help to generate an intuitive understanding of the optimal lay-up and may be used for benchmarking;
- In the case of positive shear loading of a plate with all plies having 120° orientation, the best way to improve its post-buckling resistance is to change the orientation angle of several innermost plies to the value of about 0°. The buckling level slightly decreases due to the change;
- In the case of two opposite shear loadings, the innermost layer orientation angles play an important role in improving the post-buckling performance. The best way to improve the post-buckling performance is to change the orientation angle of several innermost plies to the value of about 0°. The buckling level slightly decreases due to the change, as compared to the "equal buckling resistance" solution. The improvement of the post-buckling load-carrying capacity may reach 30-40%;
- In the case of two opposite shear loadings, there are three important fiber directions, determining the lay-up with the high buckling and post-buckling resistance. The schematic describing the lay-up construction is proposed;
- Considerable structural weight reduction opportunities are available in the case of using the proposed lay-up design approach. The opportunities are due to the improved

post-buckling behavior and nearly the same buckling resistance. The weight reduction opportunities are in the range of up to 7% and even higher.

ACKNOWLEDGEMENT

The author is grateful to colleagues for fruitful discussions and valuable remarks.

REFERENCES

[1] Bisagni C, Vescovini R. A fast procedure for the design of composite stiffened panel. Aeron J 2015, 119 (No. 212): 185-201.

[2] Turvey GJ, Marshall IH, eds. Buckling and Postbuckling of Composite Plates. London: Chapman and Hall, 1995.

[3] Wu Z, Raju G, White S, Weaver PM. Optimal design of postbuckling behavior of laminated composite plates using lamination parameters. In: 55th AIAA/ ASME/ ASCE/ AHS/ ASC Structures, Structural Dynamics, and Materials Conference, National Harbor, Maryland, USA, 2014: Paper AIAA 2014-1376.

[4] Diaconu CG, Weaver PM. Approximate solution and optimum design of compression-loaded, postbuckled laminated composite plates. AIAA J 2005, 43 (4): 906-914.

[5] Shin DS, Gürdal Z, O'Hayden G. Minimum weight design of laminated composite plates for postbuckling performance. Appl Mech Rev 1991, 44 (No. 11, part 2): S219-S231.

[6] Adali S, Verijenko VE, Walker M. Optimal laminate configurations with symmetric lay-ups for maximum post-buckling stiffness. Compos Eng 1994, 4 (No. 11): 1119-1127.

[7] Adali S, Walker M, Verijenko VE. Multiobjective optimization of laminated plates for maximum prebuckling, buckling and postbuckling strength using continuous and discrete ply angles. Compos Struct 1996, 35: 117-130.

[8] Rahman T, Ijsselmuiden ST, Abdalla MM. Postbuckling analysis of variable stiffness composite plates using a finite element-based perturbation method. Intl J Struct Stab Dynamics 2011, 11: 735- 753.

[9] Dawe DJ. Finite strip buckling and postbuckling analysis. In: Turvey GJ, Marshall IH, editors. Buckling and postbuckling of composite plates. London: Chapman and Hall, 1995. p. 108-153.

[10] Degenhardt R, Kling A, Rohwer K, Thomson RS. Design and analysis of stiffened composite panels including post-buckling and collapse. Comput & Struct 2008, 86: 919-929.

[11] Beerhorst M, Seibel M, Mittelstedt C. Fast analytical method describing the postbuckling behavior of long, symmetric, balanced laminated composite plates under biaxial compression and shear. Compos Struct 2012, 94: 2001–2009.

[12] Mittelstedt C, Erdmann H, Schröder K-U. Postbuckling of imperfect rectangular composite plates under inplane shear closed-form approximate solutions. Arch Appl Mech 2011, 81: 1409–1426.

[13] Nemoto K, Kasuya H, Kikugawa H, Asaka T. Postbuckling Behavior of Composite Laminated Plates with Initial Imperfections under Biaxial Compression. Mater Transactactions 2009, 50: 299-304.

[14] Kassapoglou C, Dobyns AL. Simultaneous cost and weight minimization of postbuckled composite panels under combined compression and shear. Struct Multidisc Optim 2001, 21: 372-382.

[15] Zhang J-W, Shen H-S. Postbuckling of orthotropic rectangular plates in biaxial compression. J Eng Mech 1991, 117: 1158-1170.

[16] Wu Z, Weaver PM, Raju G. Postbuckling optimization of variable angle tow composite plates. Compos Struct 2013, 103: 34-42.

[17] Raju G, Wu Z, Weaver PM. Buckling and postbuckling of variable angle tow composite plates under in-plane shear loading. Intl J Solids Struct, 2015, 58: 270-287.

[18] Groh RM, Weaver P. Mass optimization of variable angle tow, variable thickness panels with static failure and buckling constraints. In: 56th AIAA/ASCE/AHS/ASC Structures, Structural Dynamics, and Materials Conference, Kissimmee, Florida, USA, 5-9 January 2015.

[19] Seresta O. Buckling, flutter, and postbuckling optimization of composite structures. PhD dissertation in Aerospace Engineering. Virginia Tech., USA, 2007

[20] Fares ME, Youssif YG, Elshoraky AE. Non-linear design and control optimization of composite laminated plates with buckling and postbuckling objectives. Intl J of Non-Lin Mech 2006; 41 (6–7): 807-824.

[21] Koide RM, Lima LM, Ferreira APCS, Luersen MA. Postbuckling optimization of laminated composite rectangular plates and stiffened panel under compression using firefly algorithm. In: 24th ABCM International Congress of Mechanical Engineering. December 3-8, 2017, Curitiba, PR, Brazil.

[22] Henrichsen SR, Weaver PM, Lindgaard E, Lund E. Postbuckling Optimization of Composite Structure Using Koiter's Method. Intl J of Numer Meth in Eng 2016, 108 (8): 902–940.

[23] Hutchinson JW, Koiter WT. Postbuckling theory. Appl Mech Rev 1970, 23: 1353-1366.

[24] Kassapoglou C. Design and Analysis of Composite Structures: With Applications to Aerospace Structures. John Wiley & Sons, 2010.

[25] Washizu K. Variational Methods in Elasticity and Plasticity. 2nd ed. Oxford, New York: Pergamon Press, 1975.

[26] Gibson RF. Principles of Composite Material Mechanics. New York: McGraw-Hill, Inc., 1994.

[27] Zhang Y, Matthews FL. Postbuckling Behavior of Anisotropic Laminated Plates Under Pure Shear and Shear Combined with Compressive Loading. AIAA J. 1984; 22(2): 281-286.

[28] Grenestedt JL. Layup optimization against buckling of shear panels. Struct Multidisc Optim 1991, 3: 115-120.

[29] Selyugin S. On choice of optimal anisotropy of composite plates against buckling, with special attention to bending-twisting coupling. Struct Multidisc Optim 2013, 48: 279–294.

[30] Weaver P Anisotropic Elastic Tailoring in Laminated Composite Plates and Shells. In: Falzon BG, Aliabadi MH Buckling and postbuckling structures: experimental, analytical and numerical studies, Imperial College Press, 2008, pp 177-224.